Supporting Information

Aung et al. 10.1073/pnas.1102855108

SI Experimental Procedures

Cells, Antibodies, Small Molecules, Plasmids, and Vectors. The diffuse large B-cell lymphoma (DLBCL) cell lines Su-DHL-4 and Karpas 422 were obtained from a public depository (DSMZ). The cell line Balm-3 (1) was kindly provided by B. Glass (ASKLEPIOS Klinik St. Georg, D-20099 Hamburg, Germany), and the cell OCI-Ly1 (2) was from the Ontario Cancer Institutes (Toronto, ON Canada M5G 2M9); the cell lines were propagated in RPMI 1640 supplemented with 25 mM Hepes, GlutaMAX I (Gibco-BRL), 1× penicillin/streptomycin (Sigma and Biochrom), and 10% heat-inactivated FCS (Gibco-BRL). Approval for the collection and analysis of patient blood samples was obtained from the Institutional Review Board of the University Medicine Goettingen and was conducted according to the Declaration of Helsinki. Each patient gave specific informed consent for the procedure. Cell viability was determined using 3-(4,5-dimethylthiazol-2-yl)-2,5-diphenyltetrazolium bromide (MTT) assay as previously described (3). Briefly, cells were seeded in triplicate on 96-well culture plates at a density of 1×10^5cells/well and were treated with the indicated concentrations of specific agent and a DMSO control and then incubated at 37 °C. After 24 h, the culture volume of 100 μL was supplemented with MTT in PBS to achieve a final concentration of 0.5 mg/mL. After 4 h of incubation, suspension cells were spun, the supernatant discarded, and the pellet resuspended in 33% (vol/vol) DMSO and 5% (vol/vol) formic acid (all from Sigma) dissolved in isopropanol. The light absorbance from formazan and background was measured at 540 and 655 nm on a Tecan SLT photometer (BioRad model 680 Microplate Reader). We expressed the effect on viability as the ratio of values from treated versus untreated samples; i.e., specific viability is the ratio of absorbance with drug to absorbance of solvent control. IC_{50} was defined as the concentration of drug causing a 50% inhibition of cell growth compared with untreated control and was determined using the curve-fitting function (sigmoidal dose response, variable slope) of Graph Pad Prism version 4.03 for Windows (GraphPad Software, http://www.graphpad.com).

The primary antibodies used in this study for the applications were as indicated: therapeutic anti-CD20 rituximab (type I) and GA101 (type II, both Roche), anti-rituximab idiotype (clone MB2A4, AbD serotec), anti–flotillin-2 (clone 29, BD-Pharmingen), anti-alix (clone 49/AIP1, BD-Pharmingen), anti-CD9 (clone M-L13, BD-Pharmingen), anti-CD63 (clone H5C6, BD-Pharmingen), anti-CD55 (clone IA10, BD-Pharmingen), anti-CD59 (clone p282, BD-Pharmingen), anti-CD46 (clone E4.3, BD-Pharmingen), anti–SC5b-9 monoclonal antibody W13/15 for the detection of terminal complement complex (4), and anti-C3b/iC3b/C3dg monoclonal antibody I3/15 (5). Secondary antibodies against mouse or rabbit Ig were obtained from Santa Cruz Biotechnology.

Small molecules were used at the concentrations indicated in the figures: mTOR inhibitor rapamycin, COX-2 inhibitor indometacin, and cholesterol synthesis inhibitor U18666A (all from Sigma). Fluorescent dyes CalceinAM and PKH26 were applied (both from Molecular Probes). For silencing ABCA3, two validated specific shRNA sequences [RNAi Consortium (TRC), http://www.broadinstitute.org/rnai/trc: TRC clone ID TRCN0000059338, here referred to as shABCA3.38—forward 5′-CCGG(GCCCAGCTCATTGGGAAATTT)CTCGAG(AAATTTCCCAATGAGCTGGGC)TTTTTG-3′; reverse 5′-AATTCAAAAA(AAATTTCCCAATGAGCTGGGC)CTCGAG(GCCCAGCTCATTGGGAAATTT)-3′; and TRC clone ID TRCN0000059339, here referred to as shABCA3.39—forward 5′-CCGGGCCCAGCTCATTGGGAAATTTCTCGAGAAATTTCCCAATGAGCTGGGCTTTTTG-3′; reverse 5′-AATTCAAAAAGCCCAGCTCATTGGGAAATTTCTCGAGAAATTTCCCAATGAGCTGGGC-3′] were cloned into pLKO.1-eGF (Addgene), and lentiviral particles were produced in the HEK293T producer cell line with the plasmids pCMV-ΔR8.91 (containing *gag*, *pol*, and *rev* genes) and pMD.G (VSV-G–expressing plasmid) following standard protocols (6). For enforced expression of ABCA3 in lymphoma cells, the plasmids pEGFP-N1-ABCA3 wt and pEGFP-N1-ABCA3 N568D mutant carrying a mutation in the ATP-binding site of the transporter were used as described previously (7, 8). Briefly, for plasmid transfer, 5×10^6 cells in 180 μL OptiMEM (Gibco-BRL) were mixed in a prechilled 1.5-mL reaction tube with 30 μg of either pEGFP-N1-ABCA3 wild type or pEGFP-N1-ABCA3 N568D. A total of 100 μL of cells/plasmid mix was pulsed in a prechilled electroporation cuvette (Eppendorf) with an electroporator (Multiporator, Eppendorf) (1200 V, 100 μs) and consecutively incubated in 2 mL complete growth medium overnight. For selection, 800 mg/L G418 (Roche) were added every 3 d to complete growth medium. Cells were used for experiments when they reached exponential growth rate, with documentation of enforced ABCA3 expression by quantitative reverse transcription PCR (qRT/PCR) in comparison with wild-type controls.

Microscopy. For confocal microsocopy, cells were fixed at room temperature using 3.7% paraformaldehyde for 20 min, with the subsequent quenching of any unspecific binding using 50 mM NH_4Cl for 15 min and permeabilization with 0.05% Triton X-100 in PBS for 15 min. Primary antibodies were diluted 1:100 in PBS for 1 h. After washing twice with PBS and incubating with 10% goat serum, the primary antibodies were visualized using goat secondary antibodies at a dilution of 1:500 in PBS coupled to Cy3 (Dianova). All samples were mounted in Fluoromount (DAKO) and analyzed with the TCS-2 AOBS confocal laser scanning microscope (Leica) with a 63× inversion oil objective (Leica). The data were exported as TIFF files and arranged using Adobe PhotoShop without further modification of the primary image. Immunoelectron microscopy was performed according to the Tokuyasu method. Cell and exosome samples were fixed with 2% paraformaldehyde and 0.1% glutaraldehyde in 0.1 M sodium phosphate (pH 7.4) at room temperature for 30 min, before the cells were postfixed with 4% paraformaldehyde and 0.1% glutaraldehyde on ice for 2 h. After being washed twice with PBS–0.02% glycine, the cells were embedded in 10% gelatin, cooled on ice, and cut into small blocks. The blocks were infused with 2.3 M sucrose overnight and stored in liquid nitrogen. Ultrathin cryosections were cut from the frozen samples and labeled with primary antibodies detected with protein A conjugated to gold (PAG). In the case of monoclonal antibodies, a polyclonal rabbit anti-mouse bridging antibody (Sigma) was used before detection with PAG. Sections were contrasted with uranyl acetate methyl cellulose on ice for 10 min, embedded in the same solution, and examined with a Phillips CM120 electron microscope. In preparation of whole-cell imaging, cells were fixed in 2% glutaraldehyde in 0.1 M PBS (pH 7.4) for 2 h, postfixed in 1% OsO_4 for 1 h, dehydrated in ethanol, and then embedded in Epon.

Flow Cytometry. Detection of membrane bound fluorescence was performed using standard protocols for flow cytometry. Cells ($1 \times$ 105 per condition) were washed with PBS and incubated for

30 min at RT with either primary antibody or isotype control (both 1:50). FACS analysis of exosomal surface proteins was carried out after exosomes had been coupled to latex beads. Exosomes (40 μg protein) were incubated in 30 μL PBS with 4-μm aldehyde/sulfate latex beads (3 μL of a 4% wt/vol suspension; Invitrogen) for 15 min and again for 2 h after addition of 500 μL PBS at room temperature (RT) under constant agitation. The reaction was stopped by addition of 100 μL 1 M glycine for 30 min with gentle agitation, followed by three washes in PBS/0.5% wt/vol BSA. Antibody staining followed the protocols for antibody staining of cells in suspension.

LDS-PAGE, Western Blot, and PCR. For lithium dodecyl sulfate-polyacrylamide gel electrophoresis (LDS-PAGE), total cell lysates were prepared in CelLytic M (Sigma), supplemented with 1 mM Na_3VO_4, 10 mM Na_2MoO_4, and proteinase inhibitor mixture (Sigma). Twenty-five micrograms of protein were run on an LDS NuPage Novex 4–12% BisTris gradient gel in accordance with the manufacturer's recommendations. Protein transfer was completed using 30 V for 60 min on Hyperbond-C Extra (Amersham Biosciences) and blocked with 5% BSA (Sigma) in 0.1% Tris-buffered saline. After washing, membranes were probed against the indicated antigens following the manufacturer's recommendation for the antibodies. Secondary HRP-conjugated antibodies against anti-rabbit or anti-mouse were purchased from Santa Cruz. For chemoluminescence detection, standard ECL (Pierce) was used. For quantification of mRNA, qRT/PCR of hABCA3 and β-actin transcripts was performed in triplicate on a Taqman cycling machine (ABI Prism 7900HT Sequence Detection System, Applied Biosystems) following previously published protocols (7). Briefly, the SYBR green kit (Qiagen) was used according to the manufacturer's protocols, with 40 cycles of denaturation (15 s at 95 °C), annealing (45 s at 58 °C), and elongation (60 s at 72 °C) followed by a melting curve analysis. Subsequently, the threshold PCR cycle number (*CT*) was obtained when the increase in the fluorescence signal of the PCR product indicated exponential amplification (9). This value was normalized to the threshold PCR cycle number obtained for β-actin mRNA from a parallel sample. The hABCA3 primer (us 5′-TTCTTCACCTACATCCCCTAC-3′; ds 5-CCTTTCGCCT-CAAATTTCCC-3′) yielded an amplicon of 139 bp (10), and the β-actin primer (us 5′-CACACTGTGCCCATCTACGA-3′; ds 5′-TGAGGATCTTCATGAGCTAGTCAG-3′) yielded an amplicon of 99 bp. A dilution series of eGFP-N1 + ABCA3 (1×10^{-3} to 1×10^{-9} M (8) was run in parallel with all reactions to allow comparison.

Complement Analysis and Rituximab Measurements. To detect and quantify rituximab in medium and patient serum samples, an ELISA using the anti-idiotypic monoclonal antibody MB2A4 was applied as previously described (11). Briefly, MB2A4 was coated at a concentration of 5 μg/mL in coating buffer on 96-well plates (Medisorb, Nunc), blocked, and washed appropriately, and diluted rituximab-containing samples were added to the plate for 90 min. Following washes, the wells were incubated with anti-human Fc–horseradish peroxidase for 60 min before further washing and addition of the 3,3′,5,5′-tetramethylbenzidine (TMB) substrate solution. TMB product was measured with a microplate reader at 450/540 nm. Background values from medium or matched serum samples before rituximab addition or infusion were subtracted, and standard dilution series of rituximab were run in parallel to allow rituximab quantification. To measure CDC, rituximab was added to lymphoma cells (1×105/100 μL) in complete medium supplemented with human serum (10–20% vol/vol, as indicated) without prior heat inactivation (56 °C for 45 min). After 24 h at 37 °C, cell viability was determined in triplicates by MTT staining as described before (3). The effect on viability was expressed as the ratio of values from treated versus untreated samples; i.e., specific viability = 100 × absorbance with antibody treatment/absorbance of untreated control. To detect complement decomposition of C3 in supernatant of exosome coupled to beads, monoclonal antibody I3/I5 was coated onto 96-well Medisorp plates (NUNC, Medisorp, Thermo Fisher Scientific), blocked, and washed. Subsequently, appropriately diluted supernatant of exosome:bead complex samples was added to the plate for 60 min, washed, and incubated with rabbit anti-C3d for 60 min. Finally, anti-rabbit Fc conjugated to horseradish peroxidase was added for 60 min before washing and addition of TMB substrate solution. Zymosan (Sigma) was used for maximal complement fixation as positive control, and addition of beads without exosomes was used as negative control.

Statistical Evaluations. The indicated statistical tests were performed using GraphPad Prism version 4.03 for Windows (GraphPad Software, http://www.graphpad.com), and differences with $P < 0.05$ were considered significant, as marked by asterisks in the respective figures. Error bars represent SDs of samples.

1. Lok MS, et al. (1979) Establishment and characterization of human B-lymphocytic lymphoma cell lines (BALM-3, -4 and -5); intraclonal variation in the B-cell differentiation stage. *Int J Cancer* 24:572–578.
2. Tweeddale M, et al. (1989) Production of growth factors by malignant lymphoma cell lines. *Blood* 74:572–578.
3. Denizot F, Lang R (1986) Rapid colorimetric assay for cell growth and survival. Modifications to the tetrazolium dye procedure giving improved sensitivity and reliability. *J Immunol Methods* 89:271–277.
4. Würzner R, et al. (1991) Inhibition of terminal complement complex formation and cell lysis by monoclonal antibodies. *Complement Inflamm* 8:328–340.
5. Oppermann M, et al. (1990) Quantitation of components of the alternative pathway of complement (APC) by enzyme-linked immunosorbent assays. *J Immunol Methods* 133:181–190.
6. Stewart SA, et al. (2003) Lentivirus-delivered stable gene silencing by RNAi in primary cells. *RNA* 9:493–501.
7. Chapuy B, et al. (2008) Intracellular ABC transporter A3 confers multidrug resistance in leukemia cells by lysosomal drug sequestration. *Leukemia* 22:1576–1586.
8. Cheong N, et al. (2007) ABCA3 is critical for lamellar body biogenesis in vivo. *J Biol Chem* 282:23811–23817.
9. Livak KJ, Schmittgen TD (2001) Analysis of relative gene expression data using real-time quantitative PCR and the 2(-Delta Delta C(T)) Method. *Methods* 25:402–408.
10. Matsumura Y, Sakai H, Sasaki M, Ban N, Inagaki N (2007) ABCA3-mediated choline-phospholipids uptake into intracellular vesicles in A549 cells. *FEBS Lett* 581: 3139–3144.
11. Cragg MS, et al. (2004) A new anti-idiotype antibody capable of binding rituximab on the surface of lymphoma cells. *Blood* 104:2540–2542.

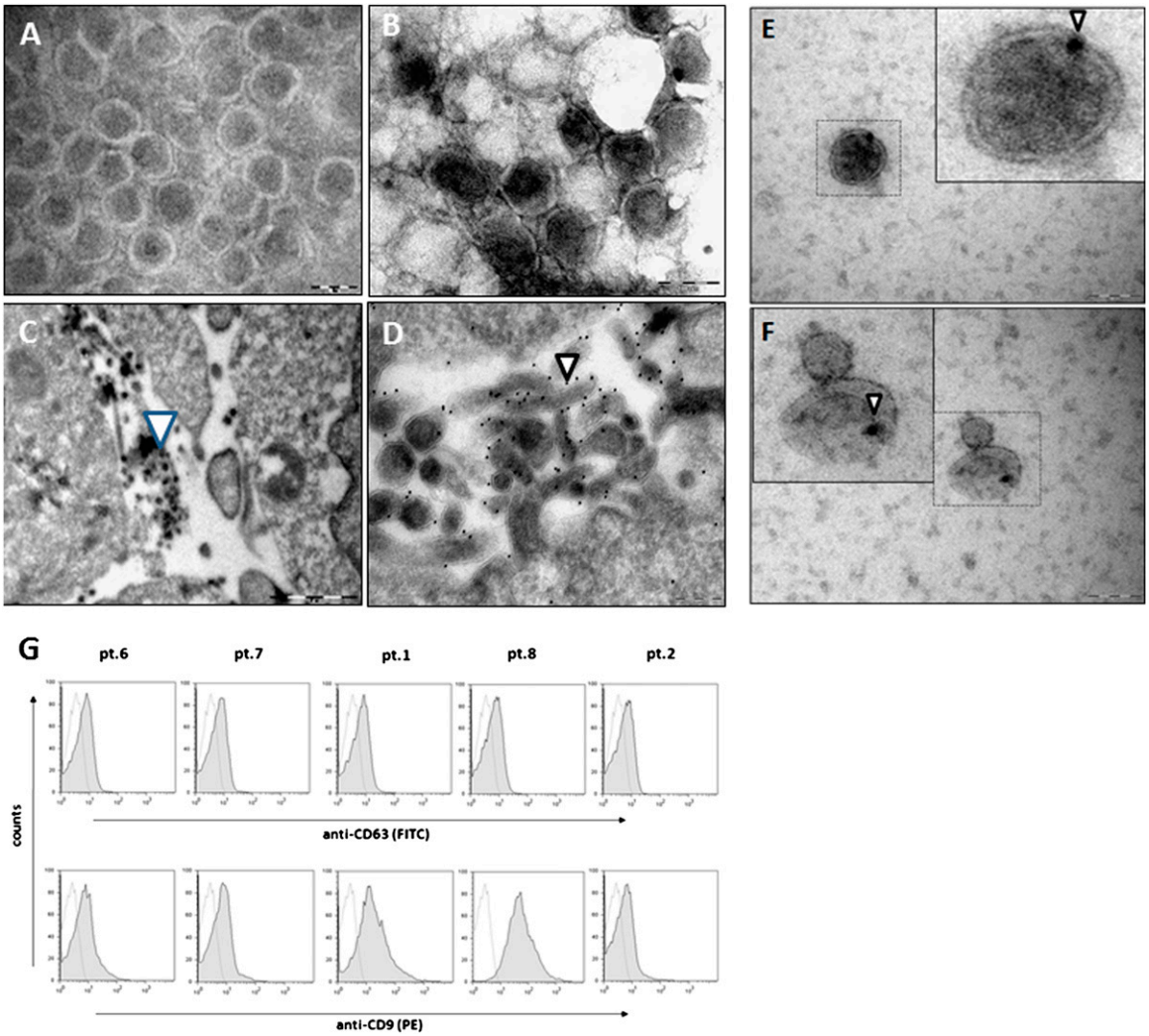

Fig. S1. Morphology and characterization of exosome preparations from aggressive B-cell lymphoma cell lines and patient samples. Differential ultracentrifugation of cell culture supernatants from B-cell lymphoma cell lines yielded monomorphic microvesicular structures with the typical size and morphology of exosomes (*A*: Su-DHL-4), similar to the exosome preparations from the erythroleukemic cell line K562 (*B*). (Scale bar, 100 nm.) Such vesicles were also found accumulating in the intercellular space between lymphoma cells (arrowhead in *C*) (Scale bar, 1 μm.) As a positive control to the binding of rituximab on exosomes shown in Fig. 1*A*, binding of the antibody was also detected by protein A–immunogold staining on the surface of plasma protrusions (*D*). (Scale bar, 200 nm.) Protein A–immunogold staining also detected binding of rituximab on the membrane of exosomes from the cell lines OCI Ly1 (*E*) and Su-DHL-4 (*F*) (compare Fig. 1*A*). Similarly, exosomes were prepared from the plasma of five representative patients with untreated lymphoma disease by ultracentrifugation (*G*). Exosomes were coupled to beads, and CD63 (*Upper* row) and CD9 (*Lower* row) surface expressions were detected by staining with FITC-labeled antibodies. The samples had been taken from four patients with DLBCL [patients (pts.) 6, 1, 8, 2] and one patient with follicular lymphoma (pt. 7).

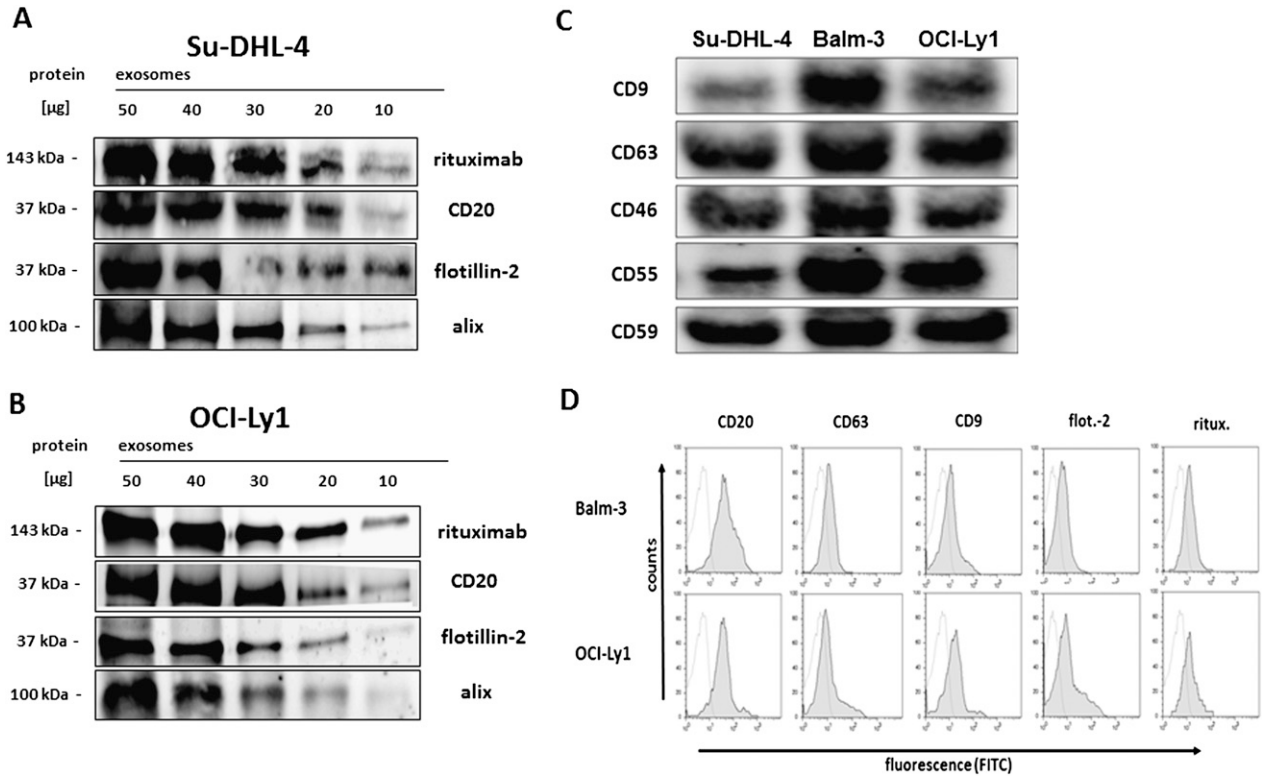

Fig. S2. Expression of exosomal marker proteins and complement regulatory proteins on lymphoma cell-derived exosomes. Supplemental to the protein expression shown in Fig. 1*B* for cell line Balm-3, expression of CD20, flotillin-2, and alix, as well as binding of rituximab were also detected in Western blots of exosomes from the cell lines Su-DHL-4 (*A*) and OCI-Ly1 (*B*). (*C*) Expression of the complement-regulating proteins CD46, CD55, and CD59, as well as the tetraspanins CD9 and CD63, was also confirmed by Western blot of exosome protein preparations for the cell lines Su-DHL-4, OCI-Ly-1, and Balm-3. (*D*) Binding of the therapeutic monoclonal antibody rituximab, as well as of CD20, flotillin-2, CD63, and CD9 on exosomes from cell lines Balm-3 and OCI-Ly1 was documented by FACS with detection of binding to purified exosome-labeled beads (for cell line Su-DHL-4, compare Fig. 1*C*).

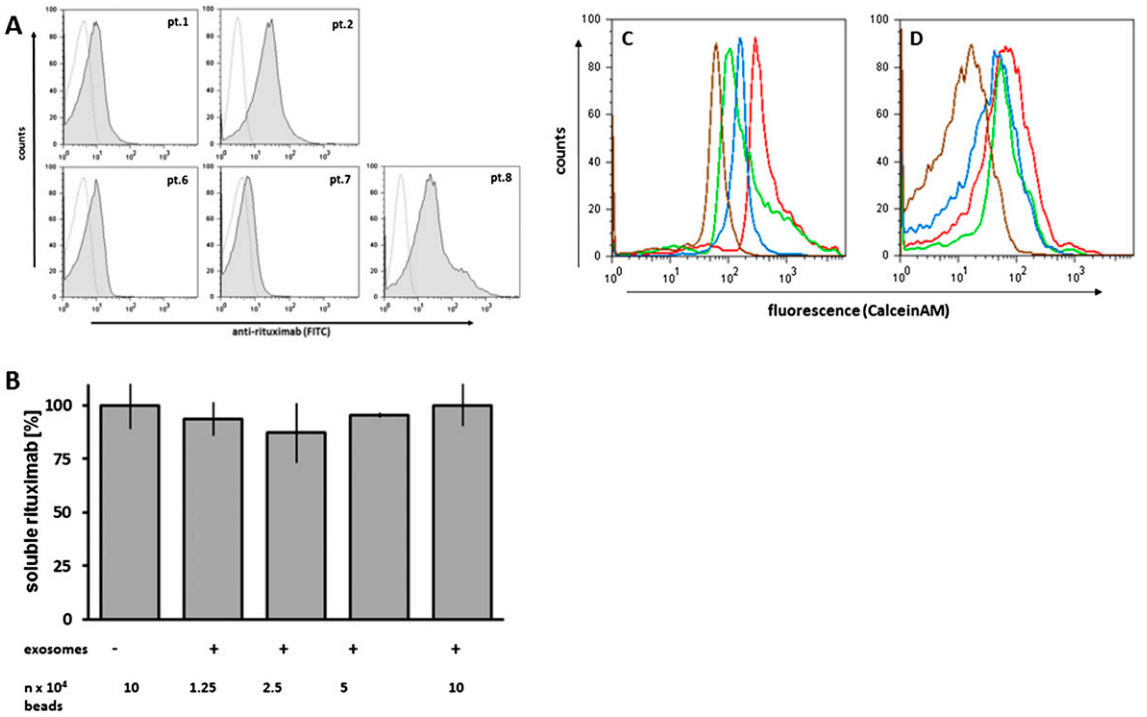

Fig. S3. (*A*) Binding of the therapeutic antibody rituximab to exosomes in vivo. Exosomes were prepared by ultracentrifugation from plasma samples of patients 3 h after the end of rituximab infusion. Exosomes were coupled to beads, and binding of rituximab was detected by staining with a FITC-labeled antibody against rituximab (MB2A4). The samples originated from four patients with DLBCL [patients (pts.) 1, 2, 6, 8], one patient with follicular lymphoma, and one patient with follicular lymphoma (pt. 7). (*B*) No absorption of anti-CD20 antibody rituximab by CD20-negative exosomes derived from K562 cells. Exosomes from K562 cells were added to medium supplemented with rituximab at an initial concentration of 35 ng/100 μL for 1 h at 21 °C. Soluble rituximab was measured by ELISA, and values were expressed as the percentage of controls treated with nonexosome-labeled beads only. Mean values of triplicates from a representative experiment are shown. (*C* and *D*) Resistance of lymphoma exosomes against rituximab-initiated complement-dependent cytolysis. Latex beads coated with exosomes of the cell lines Balm-3 (*C*) and Su-DHL-4 (*D*) were labeled with CalceinAM and analyzed by flow cytometry. Fixation of complement by exposure to rituximab in the presence of 20% active human serum for 1 h at 37 °C (blue line) decreased CalceinAM fluorescence compared with exosomes after exposure to heat-inactived serum (red line, negative control). Exposure to detergent agents (Fix&Perm, green line; SDS, brown line; both as positive controls) lysed exosomes and induced maximal liberation of CalceinAM. Complement-mediated exosome destruction (blue line) induced low-level liberation of CalceinAM in both cell lines.

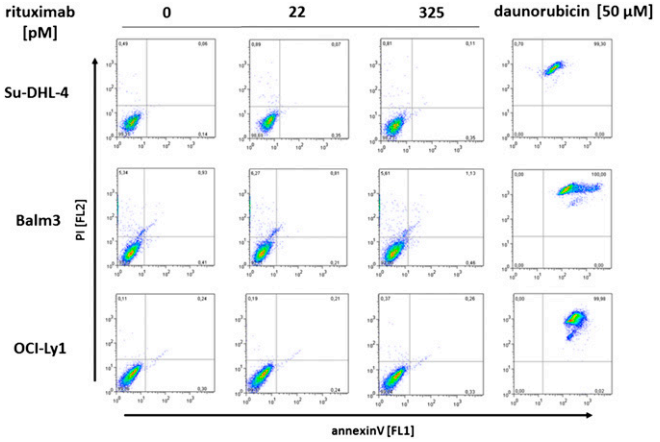

Fig. S4. Analysis of apoptosis at sublytic rituximab concentrations. Lymphoma cells were exposed to 22 and 325 pM rituximab for 4 h in the presence of complement and stained with propidium iodine (PI, *y* axis) and annexinV (*x* axis) to detect dead (i.e., PI-positive) and/or apoptotic (i.e., annexinV-positive) cells. In contrast to complete cell death induced by 50 μM daunorubicin as positive control, rituximab at these concentrations failed to induce significant apoptosis.

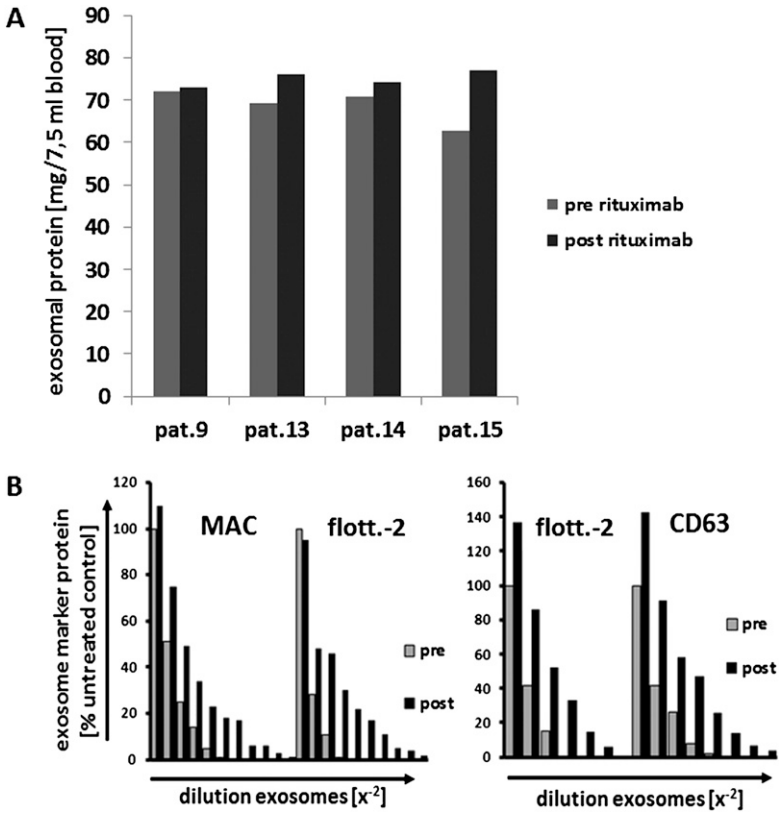

Fig. S5. Plasma exosomes in patients following therapeutic rituximab exposure. Exosomes were prepared by differential ultracentrifugation from 7.5 mL of plasma from previously untreated lymphoma patients directly before and 3 h after completed infusion of 375 mg/m^2 body-surface rituximab. Total protein of the exosome preparation (*A*, $n = 4$), as well as relative amounts of membrane attack complex (MAC), flottilin-2 (flott.-2), and CD63 (*B*, $n = 5$), were measured. The relative amounts of MAC and exosomal marker proteins were determined by diluting the exosome fractions, preparing dot blots, detecting specific antibodies, and quantifying the dot stainings with ImageJ. Both MAC and the exosomal markers were found significantly increased post rituximab infusion (*B*).

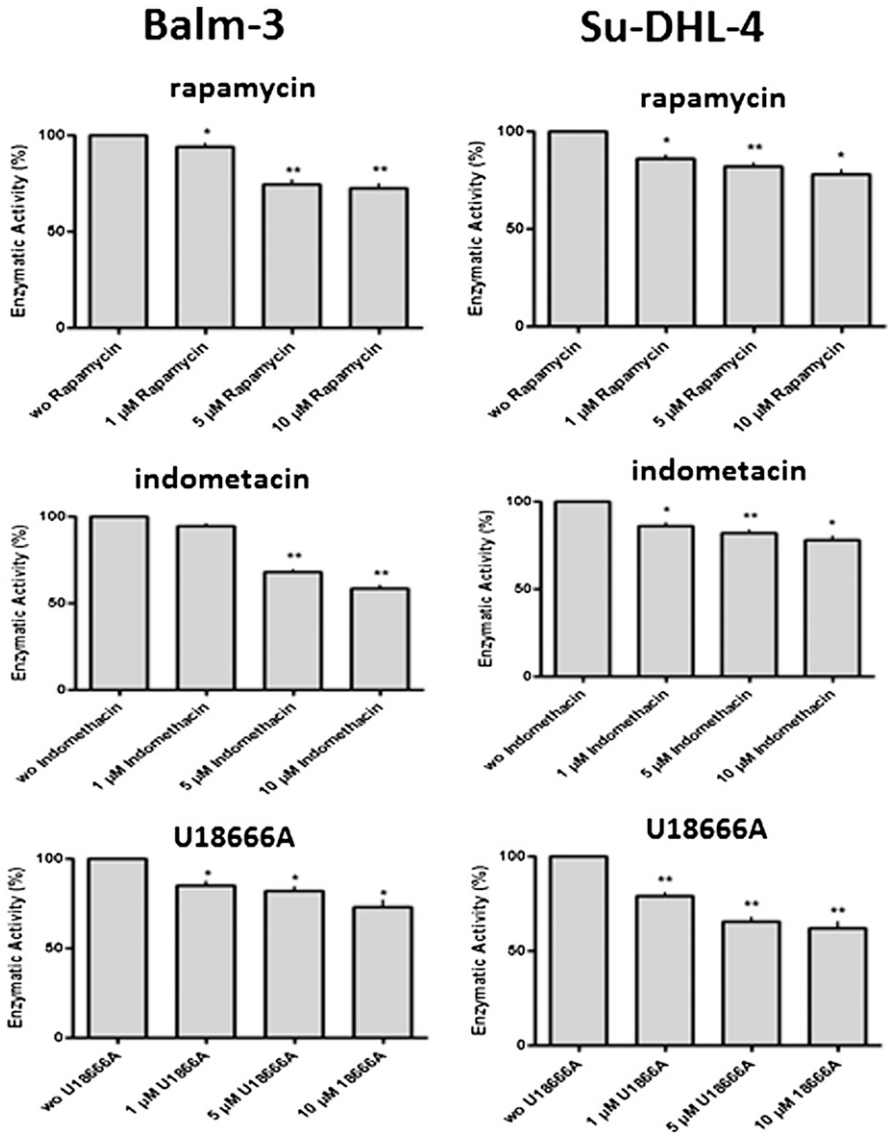

Fig. S6. Inhibition of exosome shedding from lymphoma cells. Lymphoma cells (5×10^7) were exposed to inhibitors of exosome synthesis or release at nontoxic dose ranges. Exosomes were harvested after a 24-h incubation period, and yields were measured by acetyl-cholin-esterase activity. Significant differences to controls without inhibitors (repeated measurement ANOVA with Bonferroni's post test) are marked with asterisks.

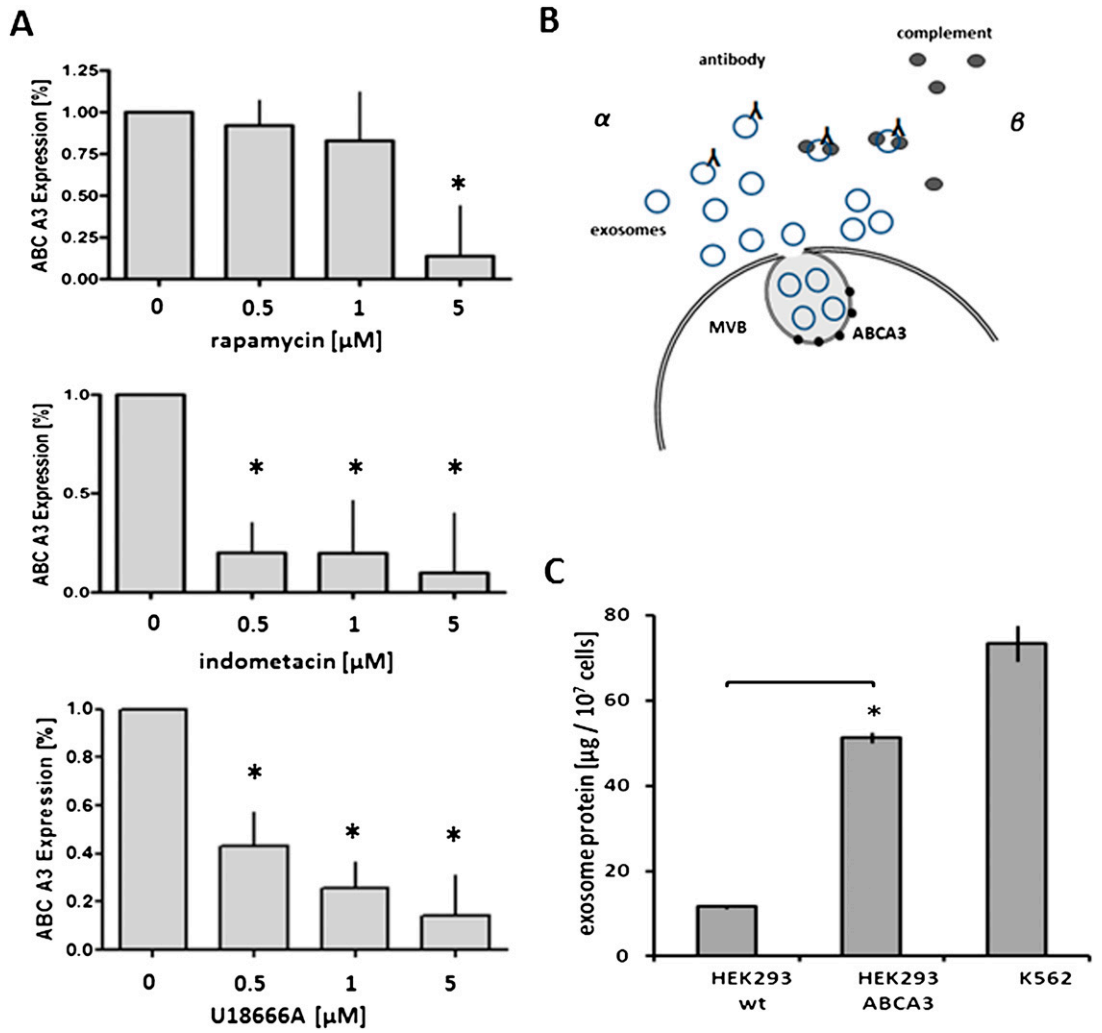

Fig. S7. (*A*) Expression of ABCA3 following incubation with rapamycin, indometacin, and U18666A. Following exposure to rapamycin, indometacin, and U18666A for 48 h at the concentrations indicated, transcript levels of ABCA3 in cell line Su-DHL-4 were determined by qRT/PCR, revealing a decrease of ABCA3 levels occurring in particular with indometacin (significant differences as tested by repeated measurement ANOVA with Dunn's post test marked by asterisks). (*B*) Schematic of the mechanisms involved in exosome-mediated protection of lymphoma cells from complement-dependent cytolysis attack. Following biogenesis in cytoplasmatic multivesicular bodies (MVB) facilitated by ABCA3, exosomes are released and shield lymphoma cells by absorption of rituximab to the CD20-positive exosomes (α) and by consumption of complement on the exosome surface (β). (*C*) Induction of increased exosome release by enforced ABCA3 expression in HEK293A cells. Addressing ABCA3 overxepression, 4×10^7 cells of HEK293A, the stable ABCA3 overexpressing cell line HEK293A-ABCA3, and K562 cells were incubated for 17 h in 36 mL of exosome-free cell culture medium, and exosome yields were measured as total exosomal protein. The exosome yields from the HEK 293A variant cell line significantly exceeded the yields from mock transduced HEK 293A cells (*C*, Student's *t* test, $P < 0.05$).

Table S1. Exosome yields from aggressive B-cell lymphoma cell lines and lymphoma samples

Cells	Protein (μg)
K562	101.0 ± 9.3
Balm-3	98.4 ± 21.3
Su-DHL-4	121.5 ± 39.0
OCI-Ly1	205.2 ± 6.3
Patient 1	137.7 ± 2.7
Patient 2	141.3 ± 7.5
Patient 3	141.6 ± 9.0

Cells (5×10^7) of each cell line or tumor single-cell suspension were incubated for 24 h in 36 mL of exosome-free cell culture medium. The supernatants were depleted of whole cells and debris by two consecutive steps of centrifugation (500 × *g* for 10 min and 10,000 × *g* for 20 min), and the exosomes were spun to pellet (100,000 × *g* for 120 min). Exosome yields are expressed as total exosomal protein. The exosome yields from aggressive lymphoma cell lines were equivalent to or higher as in the high-level exosomes producing erythroleukemic cell line K562.

Table S2. Patient characteristics

PIN	Age	Gender	Histology	Stage	IPI	Status at sample	Treatment response	Regimen
1	75	F	DLBCL	IIIAE	4	Untreated	CR	R-CHOP
2	57	F	DLBCL	IVB	4	Relapse	PD	R-DHAP
3	81	M	DLBCL	IVA	4	Untreated	PR	R-CHOP
4	45	M	DLBCL	IVA	2	Untreated	RD	R-CHOP
5	64	M	IC	IVA	NA	Untreated	PR	R-FC
6	72	M	DLBCL	IIAE	1	Untreated	CR	R-CHOP
7	64	M	FL	IVB	NA	Untreated	CRu	R-Bendamustin
8	55	M	DLBCL	IVB	2	Relapse	CRu	Allo tx
9	47	M	DLBCL	IIA	1	Untreated	NA	R-CHOP
10	72	F	MCL	IVB	NA	Untreated	NA	R-CHOP
11	46	F	MZL	IIIA	NA	Untreated	NA	R-CHOP
12	67	M	DLBCL	IAE	1	Untreated	NA	R-CHOP
13	83	F	FL	IIIB	NA	Relapse	NA	R-Bendamustin
14	72	M	DLBCL	IAE	1	Untreated	NA	R-CHOP
15	69	M	DLBCL	IBE	1	Untreated	NA	R-CHOP

Listed are the characteristics of the male (M) and female (F) lymphoma [diffuse large B-cell lymphoma (DLBCL), immunocytoma (IC), follicular lymphoma (FI), mantle cell lymphoma (MCL), marginal zone lymphoma (MZL)] patients referred to by the personal identification number (PIN) in *Results*. All patients had active disease classified in stages according to Ann Arbor staging system (stage) and the international prognostic index (IPI) at the time of blood sampling—in 12 cases naive to any immunochemotherapy (untreated) and in 3 cases in relapse before initiation of salvage therapy (relapse). Treatment responses of patients were classified as complete response (CR), complete response unconfirmed (CRu), partial response (PR), progressive disease (PD), patients under ongoing therapy are referred to as not applicable (NA). Immunochemotherapy regimens were rituximab/cyclophosphamide/doxorubicin/vincristine/prednisolone (R-CHOP), rituximab/dexamethasone/Ara-C/cisplatin (R-DHAP), rituximab/fludarabin/cyclophosphamide (R-FC), rituximab/bendamustin (R-Bendamustin), and allogeneic stem cell transplantation (Allo tx).